Nanoscale

ROYAL SOCIETY OF CHEMISTRY

PAPER

View Article Online
View Journal | View Issue

Cite this: *Nanoscale*, 2020, **12**, 20356

Fullerene nanostructures: how the oblong shape of C_{70} forms a cocrystal with an enormous asymmetric unit and related cocrystals†

Lilia M. Baldauf, Kamran B. Ghiassi, Marilyn M. Olmstead * and Alan L. Balch *

Received 7th August 2020,
Accepted 19th September 2020

DOI: 10.1039/d0nr05824f

rsc.li/nanoscale

Cocrystallization of Ni^{II}(OEP) (where OEP is the dianion of octaethylporphyrin) with C_{70} in *p*-xylene produces black plates of $12Ni^{II}(OEP)\cdot12C_{70}\cdot18$*p*-xylene (**1**). Single crystal X-ray diffraction at 90 K reveals that the crystal contains 42 individual, well-ordered molecules in the asymmetric unit with distinctive interactions between each Ni^{II}(OEP)/C_{70} pair and each pair of neighboring C_{70} molecules. Warming the crystal to 186 K produces a phase change so that only four Ni^{II}(OEP)/C_{70} sites and six *p*-xylene molecules are present. Under the same conditions Cu^{II}(OEP) cocrystallizes with C_{70} to form $Cu^{II}(OEP)\cdot C_{70}\cdot1.5$*p*-xylene (**2**) with a much simpler structure consisting of one molecule of the porphyrin and the fullerene along with 1.5 molecules of *p*-xylene in the asymmetric unit. Crystallization of C_{70} from toluene in the presence of Ni^{II}(etioporphyrin-I) produces the black solvate $6C_{70}\cdot6$toluene (**3**). It seems that C_{70} has a tendency to crystallize so that several orientations of the oblong molecule are present in the solid.

Introduction

Fullerenes, the unique molecular forms of carbon such as C_{60} and C_{70}, come in a variety of sizes and shapes.[1,2] Unlike other forms of carbon, fullerenes are soluble in a variety of organic solvents and are amenable to chemical manipulation using the tools of organic chemistry.[3,4] Both C_{60} and C_{70} have become important components in the development of bulk heterojunction (BHJ) solar cells.[5–8]

The uniform outer surfaces of fullerenes, which consist of a combination of hexagonal and pentagonal rings, frequently produce crystals that are prone to disorder as is the case with C_{60}.[9] Fortunately, fullerenes readily form cocrystals with a wide range of molecules and these cocrystals frequently have a high degree of internal order and are amenable to study by single-crystal X-ray diffraction. Such cocrystal-forming molecules include those with curved surfaces that complement the fullerene exterior.[10–12] However, molecules with flat surfaces such as porphyrins also cocrystallize with fullerenes.[13,14] Indeed, cocrystallization with M^{II}(OEP) (OEP is octaethylporphyrin) has become a routine means of crystallizing fullerenes or endohedral fullerenes for structure determinations.[15–20]

We have recently demonstrated that the metal ion in M^{II}(OEP) and the solvent used for crystallization play a significant role in determining the intermolecular structure and the stoichiometry of cocrystals formed from the nearly spherical C_{60} with I_h symmetry.[21,22] Those results led to the question of determining the factors that would determine how the oblong C_{70} molecule interacts with M^{II}(OEP) in various cocrystals. Additionally, C_{70} is the simplest of a several fullerenes with a nano-tubular shape and provides a model for what to expect from such fullerenes. Other nano-tubular carbon cages with crystallographically determined structures include $D_{5h}(1)$-C_{90},[23,24] $D_{3d}(3)$-C_{96},[25] $La_2@D_5(450)$-C_{100},[26] and $Sm_2@D_{3d}(822)$-C_{104}.[27] Understanding the nature of the fullerene/M^{II}(OEP) interaction also provides molecular models for the non-covalent bonding of porphyrins to carbon nanotubes.[28–30]

The non-polar C_{70} molecule with D_{5h} symmetry possesses a unique C_5 axis whose orientation is an excellent marker to identify the intermolecular interactions present in cocrystals. Previously, this laboratory demonstrated that C_{70} cocrystallized with bis(ethylenedithio)tetrathiafulvalene (ET) so that two different alignments of the C_5 axis of the fullerene relative to the ET molecule were observed.[31] There are two limiting orientations that the C_5 axis can have with the porphyrin plane. It may lie parallel to that plane, in which case we assign a tilt angle of 0° to the interaction. At the other extreme, the C_5 axis may be perpendicular to the porphyrin plane, in which case we assign a tilt angle of 90°. We anticipated that, by cocrystallization of C_{70} with M^{II}(OEP) with a variety of metals and utiliz-

Department of Chemistry, University of California, Davis, One Shields Avenue, Davis, CA 95616, USA. E-mail: mmolmstead@ucdavis.edu, albalch@ucdavis.edu

†CCDC 2018102–2018105. For crystallographic data in CIF or other electronic format see DOI: 10.1039/d0nr05824f

ing a variety of solvents, we would be able to obtain crystals that would have a range of intermolecular interactions between these components that could involve a range of tilt angles.

To our surprise, we discovered that in *p*-xylene, a remarkable cocrystal of C_{70} formed that displayed twelve different tilt angles with respect to Ni^{II}(OEP) in a large asymmetric unit when examined by crystallography at 90 K. When the crystal was warmed to 186 K, the unit cell volume decreased to 1/3 of the original size accompanied by fullerene disorder. An intriguing discovery was that the similar crystal growing procedure with Cu^{II}(OEP) yielded a basic unit cell containing only one formula unit of the cocrystal at 90 K and an ordered C_{70}. When C_{70} was crystallized with Ni(Etioporphyin-I), Ni(Etio-I), in toluene as the solvent, no porphyrin co-crystals formed. Instead, a structure determination at 90 K revealed six formula units of C_{70}·toluene in the asymmetric unit.

Results and discussion

Cocrystal growth

Crystals of $12Ni^{II}$(OEP)·$12C_{70}$·18*p*-xylene (**1**) and Cu^{II}(OEP)·C_{70}·1.5*p*-xylene (**2**) were prepared by layering equimolar solutions of C_{70} in *p*-xylene over a similar solution of the appropriate M^{II}(OEP) in *p*-xylene. Crystals started appearing within 72 hours but they were allowed to grow for about four weeks to achieve the size satisfactory for data collection. Crystals of $6C_{70}$·6toluene (**3**) were obtained by layering a solution of Ni^{II}(etioporphyrin-I) in benzene solution over a solution of C_{70} in toluene. Crystallographic data are listed in the Experimental section. Unit cell information can be found in the figure captions for the cocrystal structures drawings.

The structure of $12Ni^{II}$(OEP)·$12C_{70}$·18*p*-xylene (1) at 90 K. The crystals form in the space group $P\bar{1}$ with twelve molecules of C_{70}, twelve molecules of Ni^{II}(OEP) and eighteen molecules of *p*-xylene in general positions. A drawing of the asymmetric unit is shown in Fig. 1. All molecules are ordered. Each fullerene molecule is cupped by one adjacent molecule of Ni^{II}(OEP) with all eight ethyl groups embracing each fullerene. As is common with cocrystals of Ni^{II}(OEP) and fullerenes, the Ni^{II}(OEP) molecules make close face-to-face contact. In $12C_{70}$·$12Ni^{II}$(OEP)·18*p*-xylene (**1**) columns containing fullerenes and porphyrins are formed with the solvate molecules arranged at the sides of these columns. As seen in Fig. 1, the column bounded by fullerene **5** and fullerene **12** has a repeat length of 100 Å. There is a second column made up of fullerenes **1** to **4** with a shorter translational repeat. Within the columns there are close contacts between C_{70} molecules and the adjacent Ni^{II}(OEP) molecules, between back-to-back Ni^{II}(OEP) molecules and between two C_{70} molecules. The *p*-xylene molecules are arranged beside and between these columns.

There are a number of differences between the relative orientations of fullerenes and porphyrins in this unusually large array of crystalline molecules. One difference involves the tilt angle between the C_5 axis of the C_{70} molecule and the plane of the porphyrin. If the C_5 axis is parallel to the porphyrin plane that angle would be 0°, but if the fullerene stood upright so that one of the pentagons along the C_5 axis faced the porphyrin plane, that angle would be 90°. Fig. 2 shows drawings in which that angle is at a minimum (fullerene **2** with the tilt angle of only 0.3°) and at maximum (fullerene **1** with the tilt angle of 9.7°). The corresponding tilt angles of all of the 12 fullerenes are given in Table 1. For comparison, the tilt angles for other nano-tubular fullerenes are: 3.2° and 5.1° for the C_5 axis in D_{5h}(1)-C_{90}·Ni^{II}(OEP)[23] and 8.7° for the C_3 axis in D_{3d}(3)-C_{96}·$2Ni^{II}$(OEP)·$2C_6H_6$.[25] For the endohedral fullerene in La_2@D_5(450)-C_{100}·$2Ni^{II}$(OEP)·2(toluene) the tilt angle for the C_5 axis is quite large, 73.6°.[26]

A second difference involves the angle between the projection of the C_5 axis of the C_{70} molecule onto the adjacent

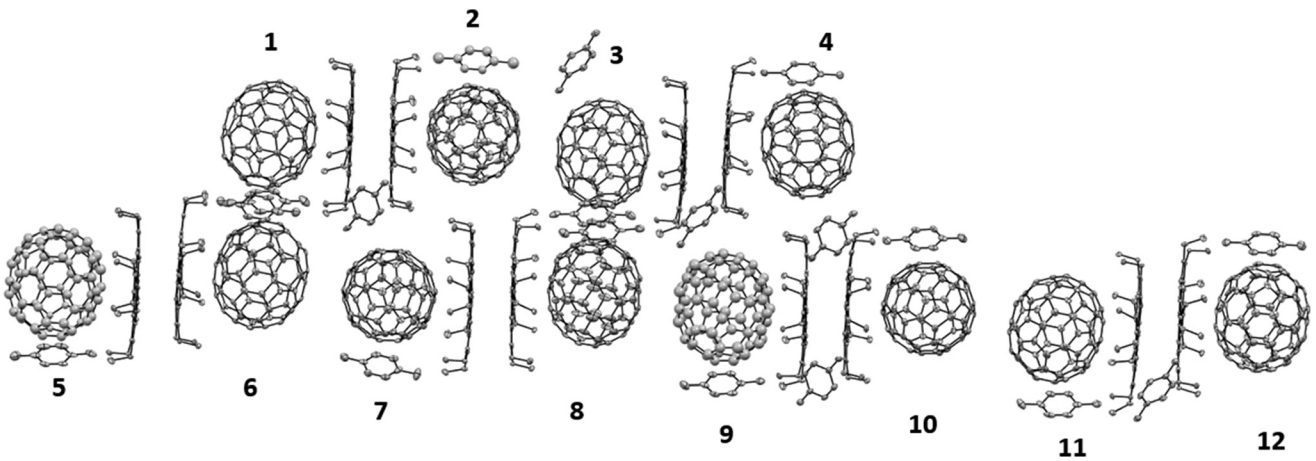

Fig. 1 A view of the unit cell contents and their relative positions in $12C_{70}$·$12Ni^{II}$(OEP)·18*p*-xylene, (**1**). Crystal data are given in Table 2. Each of the twelve different C_{70} molecules is labelled **1–12** and that label also pertains to the Ni^{II}(OEP) molecule that is adjacent to each fullerene. Hydrogen atoms have been omitted for clarity. Thermal ellipsoids are drawn at 32% probability.

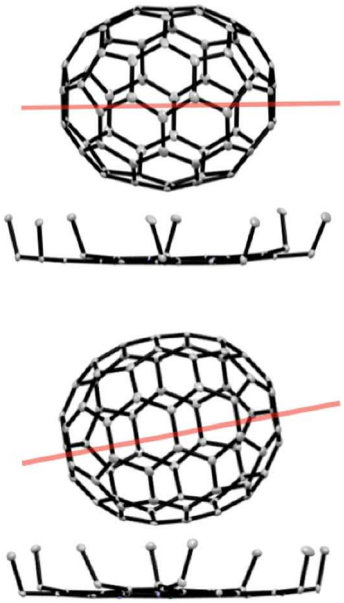

Fig. 2 Extreme relative positions of the C_5 axis in red of the fullerene and the porphyrin plane in $12C_{70}{\cdot}12Ni^{II}(OEP){\cdot}18p$-xylene, (**1**). Top; C_{70} **2** with the minimum angle, 0.3°, between the C_5 axis of the fullerene and the porphyrin plane. Bottom; C_{70} **1** with the maximum angle, 9.7°, between the C_5 axis of the fullerene and the porphyrin plane. Hydrogen atoms have been omitted for clarity. Thermal ellipsoids are drawn at 32% probability level.

Table 1 Angles (°) regarding the position of the C_5 axis in $12C_{70}{\cdot}12Ni^{II}(OEP){\cdot}18p$-xylene, (**1**)

	Tilt angle	Angle of C_5 axis relative to N–Ni–N line		Tilt angle	Angle of C_5 axis relative to N–Ni–N line
C_{70} **1**	9.7°	17.2°	C_{70} **7**	8.9°	14.3°
C_{70} **2**	0.3°	18.0°	C_{70} **8**	0.6°	22.7°
C_{70} **3**	0.9°	19.7°	C_{70} **9**	0.6°	19.3°
C_{70} **4**	7.3°	20.1°	C_{70} **10**	7.8°	13.5°
C_{70} **5**	1.9°	17.3°	C_{70} **11**	8.8°	16.5°
C_{70} **6**	8.4°	16.0°	C_{70} **12**	4.3°	22.6°

Ni^{II}(OEP) molecule and the angle that it makes from one of the N–Ni–N axes. The angle in question can take values from 0 to 45°. The angles all fall in the range 13.5 to 22.7° and are tabulated in Table 1.

Another difference involves the angle between the C_5 axes of two neighbouring C_{70} molecules. Fig. 3 shows the two extreme situations. As seen in part **A** of the figure, fullerenes **8** and **9** are aligned nearly parallel to one another with an angle of only 0.2° between the C_5 axes of the fullerenes. However, as seen in part B, fullerenes **6** and **7** are arranged so that the angle between the two C_5 axes is 73.8°. The corresponding angles between the C_5 axes of all of pairs of neighbouring fullerenes are: **1** and **4**, 16.2°; **2** and **3**, 49.6°; **5** and **12**, 2.5°; **6** and **7**, 73.8°; **8** and **9**, 0.2°; **10** and **11**, 66.3°.

As Fig. 4 shows, in $12C_{70}{\cdot}12Ni^{II}(OEP){\cdot}18p$-xylene (**1**) the porphyrin rings are not entirely planar, but show varied distor-

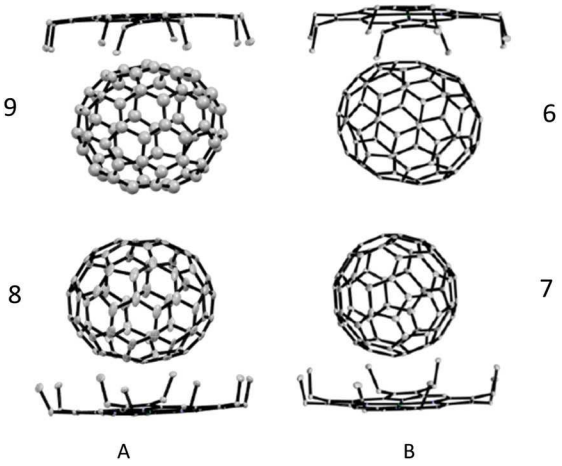

Fig. 3 Extreme relative orientations of adjacent C_{70} molecules in $12C_{70}{\cdot}12Ni^{II}(OEP){\cdot}18p$-xylene, (**1**). A; C_{70} **8** and **9** with the minimum angle of 0.2° between the C_5 axes of the fullerenes. B; C_{70} **6** and **7** an angle of 73.8° between the two C_5 axes of the fullerenes. Hydrogen atoms have been omitted for clarity. Thermal ellipsoids are drawn at 32% probability level.

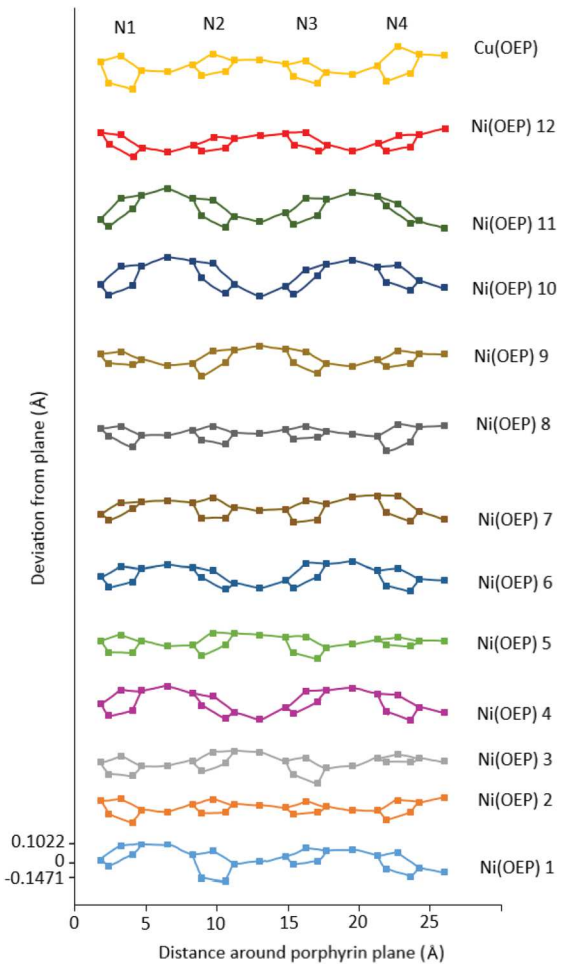

Fig. 4 Comparison of the out-of-plane displacements of the porphyrin core atoms from the mean porphyrin plane as visualized in a linear fashion for the twelve Ni^{II}(OEP) molecules in $12C_{70}{\cdot}12Ni^{II}(OEP){\cdot}18p$-xylene, (**1**) at 90 K and for Cu^{II}(OEP) in $Cu^{II}(OEP){\cdot}C_{70}{\cdot}1.5p$-xylene (**2**).

tions from planarity. In the chart below, the distances in Å of the core carbon and nitrogen atoms from the mean plane of the porphyrin are shown along the vertical axis while the individual atoms are shown in linear fashion along the horizontal axis. Such distortions of the porphyrin macrocycle have been classified as domed, saddled, ruffled, waved or pyrrole propellered.[32] The most common form of distortion seen in $12C_{70}{\cdot}12Ni^{II}(OEP){\cdot}18p$-xylene (**1**) is a slight doming seen in all except for porphyrins **6**, **10** and **11**.

The transformation of $12Ni^{II}(OEP){\cdot}12C_{70}{\cdot}18p$-xylene (1) at 186 K. Upon warming, crystals of $12Ni^{II}(OEP){\cdot}12C_{70}{\cdot}18p$-xylene (**1**) undergo a phase change. The structure of a crystal at 186 K has been determined by single crystal X-ray diffraction. At 186 K crystals are still triclinic with the same space group, $P\bar{1}$, but the lengths of *a* and *b* axes have decreased, and the unit cell volume has decreased by a factor of 33.7%. As shown in Fig. 5, the unit cell now consists of four C_{70} molecules, four molecules of $Ni^{II}(OEP)$ and six molecules of *p*-xylene. The porphyrin and *p*-xylene molecules are ordered, but each of the four sites for C_{70} molecules has a 50 : 50 occupation of two cage orientations.

The matrix for the low temperature → high temperature phase transition is

$$\begin{pmatrix} -0.333 & 0 & 0.333 \\ 0.667 & 0 & 0.333 \\ 0 & 1 & 0 \end{pmatrix}$$

Thus, the *b* axis at low temperature becomes the *c* axis at high temperature. A set of three full occupancy C_{70} molecules in the structure at low temperature becomes a set of two of the half-occupancy C_{70} molecules at high temperature. It is possible to compute that the sets of C_{70} molecules (**2**, **7**, **10**); (**4**, **5**, **12**); (**1**, **8**, **9**) and (**3**, **6**, **11**) at low temperature become new C_{70} molecules (**1**, **2**); (**7**, **8**); (**5**, **6**) and (**3**, **4**), respectively, at higher temperature. Since both porphyrin and *p*-xylene species are ordered at both temperatures, it is obvious that is the order-disorder phase change primarily involves reorientation of the C_{70} cages. A second crystal was mounted and the reversibility of the phase change was confirmed.

The structure of $Cu^{II}(OEP){\cdot}C_{70}{\cdot}1.5p$-xylene (2). Under the same conditions used to crystallize $12Ni^{II}(OEP){\cdot}12C_{70}{\cdot}18p$-xylene (**1**) but substituting $Cu^{II}(OEP)$ for $Ni^{II}(OEP)$ produces $Cu^{II}(OEP){\cdot}C_{70}{\cdot}1.5p$-xylene (**2**), which has a rather simple structure. $Cu^{II}(OEP){\cdot}C_{70}{\cdot}1.5p$-xylene (**2**) crystallizes in the triclinic space group $P\bar{1}$ with just one molecule of $Cu^{II}(OEP)$, one molecule of C_{70}, and 1.5 molecules of *p*-xylene in the asymmetric unit. Fig. 6 shows the interrelationship between the porphyrin and the fullerene. As usual, all eight ethyl groups surround the fullerene. The copper ion protrudes slightly on the side of the porphyrin that is away from the fullerene. The tilt angle of the C_5 axis relative to the porphyrin plane is 5.1°. Fig. 7 shows the unit cell and the packing of the molecules. Two $Cu^{II}(OEP)$ molecules come together in a back-to-back fashion, similar to the situation in $12Ni^{II}(OEP){\cdot}12C_{70}{\cdot}18p$-xylene (**1**). Notice that the $12Ni^{II}(OEP){\cdot}12C_{70}{\cdot}18p$-xylene(**1**) crystal and the $Cu^{II}(OEP){\cdot}C_{70}{\cdot}1.5p$-xylene (**2**) crystal form with the same ratios of components but the former has twelve independent versions of the three component molecules while the latter has just one.

Origin of the structural complexity of $12Ni^{II}(OEP){\cdot}12C_{70}{\cdot}18p$-xylene (1). What is the cause of what we are seeing in this very

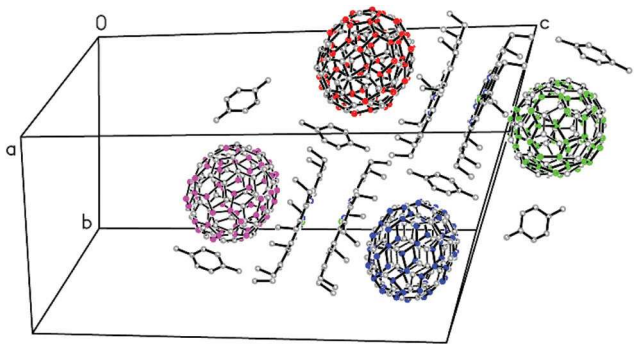

Fig. 5 A view of the asymmetric unit in $12C_{70}{\cdot}12Ni^{II}(OEP){\cdot}18p$-xylene, (**1**) at 190 K Crystal data are given in Table 2. Four ordered molecules of $Ni^{II}(OEP)$ and six ordered molecules of *p*-xylene are present. Each of the four fullerene sites is occupied by two C_{70} molecules, one of which is shown as coloured spheres. The other C_{70} molecule at that site is represented by open circles. Hydrogen atoms have been omitted for clarity.

Fig. 6 The relationship between the porphyrin and the fullerene in $Cu^{II}(OEP){\cdot}C_{70}{\cdot}1.5p$-xylene (**2**). Crystal data are given in Table 2. The solvate molecules, hydrogen atoms and minor disorder in one of the ethyl groups have been omitted for clarity. Thermal ellipsoids are drawn at the 50% probability level.

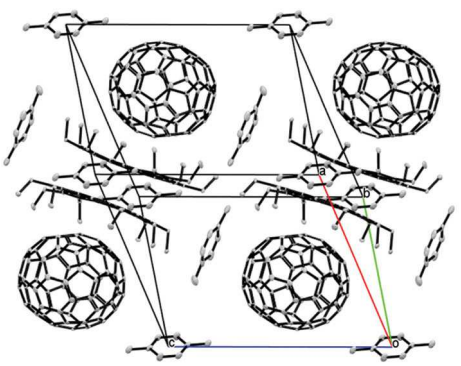

Fig. 7 The molecular packing in $Cu^{II}(OEP){\cdot}C_{70}{\cdot}1.5p$-xylene (**2**). Disordered solvent and hydrogen atoms have been omitted for clarity. Thermal ellipsoids are drawn at the 50% probability level.

large structure of C_{70}-containing molecules? Evidently, there is a distribution of multiple shallow energy conformations that occur due to the non-covalent interactions between the species in this structure. At 90 K, we can clearly observe a range of tilt angles between the plane of the porphyrin and the 5-fold rotation axis of C_{70}. This suggests that the weak π···π interactions and weak electrostatic interactions between the Ni metal and the fullerene are of primary importance. At 186 K, the intermolecular forces are a continuous influence on the crystal structure. The tilt angles do not vary greatly amongst the partially occupied fullerenes, and do not exceed nor fall below the tilt angles of the 90 K structure. The sensitivity of these interactions in driving differences in the crystallization of fullerenes in fullerene/porphyrin co-crystals is well documented.[21] Since C_{70} has a lower point group symmetry (D_{5h}) than C_{60} (I_h) we can expect a wider range of these interactions in C_{70}. In the case of $12Ni^{II}(OEP)\cdot12C_{70}\cdot18p$-xylene (**1**), there are 12 different arrangements that are not due to the inversion symmetry of the unit cell. They are distinguished according to their small intermolecular energy differences. This occurrence has been termed modulation,[33,34] and it is far more common now than in earlier days of crystallography, no doubt because of the much more common use of low temperatures. The 90 K structure is said to have $Z' = 12$, the number of symmetry-independent formula units. At 186 K, $Z' = 4$ because the different energy sets have sorted into four groups of three. We might project that $Z' = 1$ at even higher temperatures, yielding a Ni^{II} mimic of the basic structure ($Z' = 1$) of $Cu^{II}(OEP)\cdot C_{70}\cdot1.5p$-xylene. The reason for the difference between the nickel and copper structures is not obvious, but it is known that very small changes are capable giving very different results in these structures.

The structure of the solvate, $6C_{70}\cdot6$toluene (3). This solvate crystallizes in the monoclinic space group $P2_1/c$. It contains six C_{70} molecules and six toluene molecules in the asymmetric unit. Fig. 8 shows a view of the asymmetric unit. Notice that each oblong C_{70} molecule adopts a unique orientation within this unit. The six C_{70} molecules shown in Fig. 8 lie in a plane with a layer of toluene molecules positioned below them. The molecular packing can be seen in Fig. 9. Of the six independent C_{70} molecules, two have 80 : 20 disorder, only the major sites are shown in Fig. 8. Fig. 9 shows the disorder in two of the C_{70} sites.

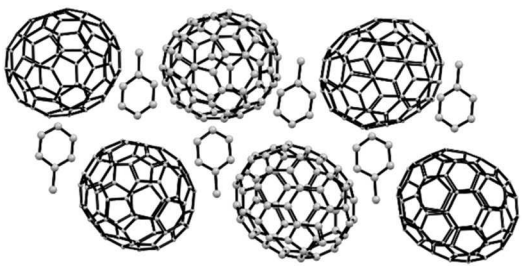

Fig. 8 The asymmetric unit in the solvate, $6C_{70}\cdot6$toluene (**3**). The six fullerenes lie in a common plane with the toluene molecules in a layer below. Crystal data are given in Table 2. Hydrogen atoms have been omitted for clarity. Thermal ellipsoids are drawn at the 32% probability level.

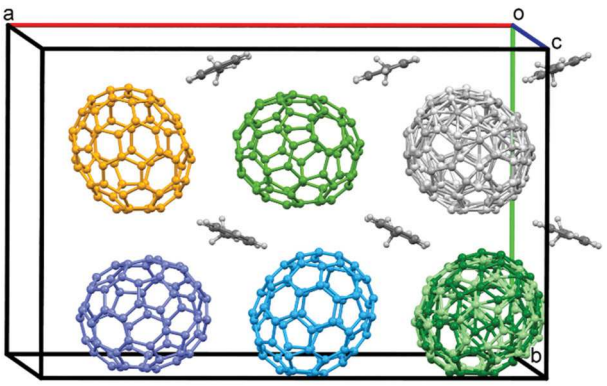

Fig. 9 Molecular packing in the solvate, $6C_{70}\cdot6$toluene (**3**) looking down the *c* axis. Each distinct C_{70} is given a unique color, and the disorder in two of the C_{70} molecules is shown. Atoms are drawn as spheres with an arbitrary radius.

Conclusions

Two new cocrystals, $12C_{70}\cdot12Ni^{II}(OEP)\cdot18p$-xylene (**1**) and $6C_{70}\cdot6$toluene (**3**), have been discovered in which the oblong C_{70} molecule adopts several different orientations to produce remarkably complex solids. Somewhat surprisingly, these complex solids are formed from three relatively rigid molecules. C_{70}, *p*-xylene and toluene have very well defined shapes and lack flexibility. $Ni^{II}(OEP)$ has some degree of flexibility in that it can distort from planarity as is seen in the four polymorphs it forms.[21,35–38] However as seen in Fig. 4, each $Ni^{II}(OEP)$ in $12C_{70}\cdot12Ni^{II}(OEP)\cdot18p$-xylene (**1**) is nearly planar and avoids the marked saddle distortion seen for the tetragonal polymorph.[33] The ethyl groups in $Ni^{II}(OEP)$ do have the opportunity to adopt different orientations about the porphyrin plane. Nevertheless, in $12C_{70}\cdot12Ni^{II}(OEP)\cdot18p$-xylene (**1**) all ninety-six ethyl groups are positioned on one side of the porphyrin plane to embrace the adjacent C_{70} molecule. While such embraces are common in cocrystals of $M^{II}(OEP)$ and various fullerenes,[15–20] there are many situations where some of the ethyl groups do not lie on the same side of the porphyrin and next to the fullerene. For example, in $Ni^{II}(OEP)\cdot C_{60}\cdot2C_6H_6$ only four of the ethyl groups surround the C_{60} molecule.[39] The other four lie on the opposite side of the porphyrin plane and do not interact with a fullerene. In $6Zn^{II}(OEP)\cdot5C_{60}\cdot5CH_2Cl_2$ of the twenty-four ethyl groups in the asymmetric unit, there is one that is turned away from embracing a C_{60} molecule.[21] In $D_{5h}(1)$-$C_{90}\cdot Ni^{II}(OEP)$, one $Ni^{II}(OEP)$ molecule has four ethyl groups embracing a C_{90} molecule on one side and the other four embracing a C_{90} molecule on the opposite side. A second $Ni^{II}(OEP)$ has the ethyl arms arranged in a two up, one down, one up, two down, one up, one down fashion with each arm near a C_{90} molecule.[23]

There are a few other cases where cocrystallization of a fullerene with $M^{II}(OEP)$ produces crystals with more than one molecule of the fullerene in the asymmetric unit. In $6Co^{II}(OEP)\cdot5C_{60}\cdot5CH_2Cl_2$ and $6Zn^{II}(OEP)\cdot5C_{60}\cdot5CH_2Cl_2$ there

are three independent C_{60} molecules in the asymmetric unit.[21] In $Sc_2(\mu_2\text{-}S)@C_s(6)\text{-}C_{82}\cdot Ni^{II}(OEP)\cdot 2C_6H_6$ there are two independent molecules of the endohedral fullerene present, one of which is fully ordered including the position of the $Sc_2(\mu_2\text{-}S)$ group inside.[40]

It is fortunate that cocrystallization of fullerenes and M^{II}(OEP) usually produces relatively straightforward structures like that of $Cu^{II}(OEP)\cdot C_{70}\cdot 1.5p$-xylene (**2**) with only one fullerene site. Such relatively simple cocrystals allow the structure of a new fullerene component to be fully investigated and ascertained, as has been done repeatedly.[15–20]

Experimental

Materials and general consideration

Ni^{II}(OEP) and H_2(OEP) were purchased from Frontier Scientific. Metalation of H_2(OEP) was accomplished by an established route.[41] C_{70} was purchased from SES Research with 99% purity. Solvents were obtained commercially and used as received. Etioporphyin-I was purchased from Frontier Scientific with 95% purity. Ni^{II}(Etio-I) was prepared according to literature methods by reacting the free-base etioporphyrin-I with nickel(II) acetate.[42,43]

Crystal growth

Procedure for $12Ni^{II}(OEP)\cdot 12C_{70}\cdot 18p$-xylene (1) and $Cu^{II}(OEP)\cdot C_{70}\cdot 1.5p$-xylene (2). In a clean scintillation vial, a 0.00168 mmol solution of C_{70} in *p*-xylene was prepared by sonication for approximately 30 minutes. In a separate scintillation vial, an equal volume of a 0.00168 mmol solution of M^{II}(OEP) in *p*-xylene was prepared. Cocrystallization was conducted in sterile, thick-walled glass tubes with an approximate inner volume of 2.0 mL. A 1.0 mL portion of the M^{II}(OEP) solution in *p*-xylene was slowly pipetted into the tube through a filter-pipet. Next, 1.0 mL of the C_{70} solution in *p*-xylene was carefully layered over the M^{II}(OEP) solution through a fresh filter pipet. The crystal tubes were capped with a rubber septum and left undisturbed in a dark cabinet until suitable crystal growth occurred. Crystal growth occurred in as little as 72 hours but crystals were allowed to grow for up to three months before they were harvested for data collection.

Procedure for $6C_{70}\cdot 6$toluene (3). In a clean scintillation vial, a 0.017 mmol solution of C_{70} in toluene was prepared by sonication for approximately 30 minutes. In a separate scintillation vial, an equal volume of 0.0868 mmol solution of nickel etioporphyrin(I) in toluene was prepared by sonication for 30 minutes. Cocrystallization was conducted in sterile, thick-walled glass tubes with an approximate inner volume of 2.0 mL. A 1.0 mL portion of the C_{70} solution in toluene was slowly pipetted into the tube through a filter-pipet. Next, 1.0 mL of the etioporphyrin-1 nickel solution in toluene was slowly pipetted into the tube through a fresh filter pipet. The crystal tubes were capped with a rubber septum and left undisturbed in a dark cabinet. Suitable crystals for data collection formed after eight months of growth.

Crystal structure determination

A black plate of $12Ni^{II}(OEP)\cdot 12C_{70}\cdot 18p$-xylene (**1**) was mounted in the 90 K nitrogen cold stream provided by a CRYO Industries low-temperature apparatus on a Bruker D8 DUO instrument equipped with a molybdenum microsource (λ =

Table 2 Cocrystal data

	$12Ni^{II}(OEP)\cdot 12C_{70}\cdot 18p$-xylene (**1**) at 90 K	$4Ni^{II}(OEP)\cdot 4C_{70}\cdot 6p$-xylene (**1**) at 186 K	$Cu^{II}(OEP)\cdot C_{70}\cdot 1.5p$-xylene (**2**) at 90 K	$6C_{70}\cdot 6$toluene (**3**) at 90 K
Chemical formula	$C_{118}H_{59}N_4Ni$	$C_{118}H_{59}N_4Ni$	$C_{118}H_{44}N_4Cu$	$C_{77}H_{88}$
Formula weight	1591.40	1591.40	1598.06	932.83
Crystal system	Triclinic	Triclinic	Triclinic	Monoclinic
Space group	$P\bar{1}$	$P\bar{1}$	$P\bar{1}$	$P2_1/c$
T (K)	90 (2)	186 (2)	90 (2)	90 (2)
a (Å)	35.187 (4)	17.1062 (10)	15.2358 (4)	32.398 (6)
b (Å)	35.564 (4)	25.9900 (15)	15.8431 (4)	21.103 (4)
c (Å)	35.852 (4)	35.865 (2)	16.7025 (4)	32.293 (6)
α (°)	102.301 (2)	107.0885 (11)	76.7210 (10)	90
β (°)	92.802 (2)	90.3877 (11)	72.5020 (10)	90.006 (3)
γ (°)	101.834 (2)	108.0069 (10)	68.6150 (10)	90
V (Å^3)	42 702 (8)	14 410.9 (14)	3548.20 (16)	22 079
Z	24	8	2	24
Reflections collected	522 801	116 981	111 006	398 191
Data/parameters/restraints	176 272/11 934/3186	74 615/5053/5040	16 311/1113/0	81 001/2904/1488
R(int)	0.1029	0.0406	0.0607	0.1452
R_1 [data with $I > 2\sigma(I)$][a]	0.1084 [80 841]	0.1186 [46 461]	0.0427 [14 011]	0.0861 [60 597]
wR_2 (all data)	0.3642	0.3438	0.1108	0.2956

[a]

$$R_1 = \frac{\Sigma||F_0| - |F_c||}{\Sigma|F_0|};\ wR_2 = \left\{\frac{\Sigma\left[w(F_0^2 - F_c^2)^2\right]}{\Sigma\left[w(F_0^2)^2\right]}\right\}^{1/2}.$$

0.71073 Å). A different crystal of (**1**) was mounted in a 186 K nitrogen cold stream on the same instrument. To determine the topotactic transformation previously discussed, the crystal of (**1**) run at 186 K was cooled to 90 K following the higher temperature run. Data for Cu^{II}(OEP)·C_{70}·1.5*p*-xylene (**2**) (black plate) were obtained similarly. A black block of $6C_{70}$·6toluene (**3**) was mounted on a Bruker Apex II diffractometer employing a fine-focus Mo sealed tube, (λ = 0.71073 Å). All data sets were reduced with the use of Bruker SAINT,[44] and a multi-scan absorption correction was applied with the use of SADABS. Structure solutions and refinements were conducted with SHELXT-2015[45] and SHELXL-2018,[46] respectively. Crystallographic data have been provided† and are reported in Table 2.

Conflicts of interest

The authors have no conflicts of interest to declare.

Acknowledgements

L. M. B. would like to thank the NSF-AGEP program for financial support. We thank the National Science Foundation for financial support (Grant CHE-1807637 to A. L. B. and M. M. O.).

References

1 H. W. Kroto, J. R. Heath, S. C. O'Brien, R. F. Curl and R. E. Smalley, *Nature*, 1985, **318**, 162–163.
2 P. W. Fowler and D. E. Manolopoulos, *An Atlas of Fullerenes*, Dover Publications, 2007.
3 W. Krätschmer, L. D. Lamb, K. Fostiropoulos and D. R. Huffman, *Nature*, 1990, **347**, 354–358.
4 A. Hirsch and M. Bretteich, *Fullerenes: Chemistry and Reactions*, Wiley-VCH, 2005.
5 J. C. Hummelen, B. W. Knight, F. LePeq, F. Wudl, J. Yao and C. L. Wilkins, *J. Org. Chem.*, 1995, **60**, 532–538.
6 S. H. Park, A. Roy, S. Beaupré, S. Cho, N. Coates, J. S. Moon, D. Moses, M. Leclerc, K. Lee and A. J. Heeger, *Nat. Photonics*, 2009, **3**, 297–303.
7 M. M. Wienk, J. M. Kroon, W. J. H. Verhees, J. Knol, J. C. Hummelen, P. A. van Hal and R. A. J. Janssen, *Angew. Chem., Int. Ed.*, 2003, **42**, 3371–3375.
8 R. Ganesamoorthy, G. Sathiyan and P. Sakthivel, *Sol. Energy Mater. Sol. Cells*, 2017, **161**, 102–148.
9 H.-B. Bürgi, E. Blanc, D. Schwarzenbach, S. Liu, Y.-J. Lu, M. M. Kappes and J. A. Ibers, *Angew. Chem., Int. Ed. Engl.*, 1992, **31**, 640–643.
10 A. S. Filatov, M. V. Ferguson, S. N. Spisak, B. Li, C. F. Campana and M. A. Petrukhina, *Cryst. Growth Des.*, 2014, **14**, 756–762.
11 K. B. Ghiassi, S. Y. Chen, P. Prinz, A. de Meijere, M. M. Olmstead and A. L. Balch, *Cryst. Growth Des.*, 2014, **14**, 4005–4010.
12 B. T. King, M. M. Olmstead, K. K. Baldridge, B. Kumar, A. L. Balch and J. A. Gharamaleki, *Chem. Commun.*, 2012, **48**, 9882–9884.
13 M. M. Olmstead, D. A. Costa, K. Maitra, B. C. Noll, S. L. Phillips, P. M. Van Calcar and A. L. Balch, *J. Am. Chem. Soc.*, 1999, **121**, 7090–7097.
14 P. D. W. Boyd, M. C. Hodgson, C. E. F. Rickard, A. G. Oliver, L. Chaker, P. J. Brothers, R. D. Bolskar, F. S. Tham and C. A. Reed, *J. Am. Chem. Soc.*, 1999, **121**, 10487–10495.
15 S. Stevenson, G. Rice, K. Harich, F. Cromer, M. R. Jordan, J. Craft, E. Hadju, R. Bible, M. M. Olmstead, K. Maitra, A. J. Fisher, A. L. Balch and H. C. Dorn, *Nature*, 1999, **401**, 55–57.
16 M. M. Olmstead, A. de Bettencourt-Dias, J. C. Duchamp, S. Stevenson, H. C. Dorn and A. L. Balch, *J. Am. Chem. Soc.*, 2000, **122**, 12220–12226.
17 S. Hu, P. Zhao, W. Shen, M. Ehara, Y. Xie, T. Akasaka and X. Lu, *Inorg. Chem.*, 2020, **59**, 1940–1946.
18 S. Stevenson, A. J. Rothgeb, K. R. Tepper, J. Duchamp, H. C. Dorn, X. B. Powers, M. Roy, M. M. Olmstead and A. L. Balch, *Chem. – Eur. J.*, 2019, **25**, 12545–12551.
19 P. Yu, W. Shen, L. Bao, C. Pan, Z. Slanina and X. Lu, *Chem. Sci.*, 2019, **10**, 10925–10930.
20 J. Zhuang, L. Abella, D.-C. Sergentu, Y.-R. Yao, M. Jin, W. Echegoyen, J. Autschbach and N. Chen, *J. Am. Chem. Soc.*, 2019, **141**, 20249–20260.
21 M. Roy, M. M. Olmstead and A. L. Balch, *Cryst. Growth Des.*, 2019, **19**, 6743–6751.
22 M. Roy, I. D. Diaz Morillo, X. B. Carroll, M. M. Olmstead and A. L. Balch, *Cryst. Growth Des.*, 2020, **20**, 5596–5609.
23 H. Yang, C. M. Beavers, Z. Wang, A. Jiang, Z. Liu, H. Jin, B. Q. Mercado, M. M. Olmstead and A. L. Balch, *Angew. Chem., Int. Ed.*, 2010, **49**, 886–890.
24 F. L. Bowles, B. Q. Mercado, K. B. Ghiassi, S. Y. Chen, M. M. Olmstead, H. Yang, Z. Liu and A. L. Balch, *Cryst. Growth Des.*, 2013, **13**, 4591–4598.
25 H. Yang, H. Jin, Y. Che, B. Hong, Z. Liu, J. A. Gharamaleki, M. M. Olmstead and A. L. Balch, *Chem. – Eur. J.*, 2012, **18**, 2792–2796.
26 C. M. Beavers, H. Jin, H. Yang, Z. Wang, X. Wang, H. Ge, Z. Liu, B. Q. Mercado, M. M. Olmstead and A. L. Balch, *J. Am. Chem. Soc.*, 2011, **133**, 15338–15341.
27 B. Q. Mercado, A. Jiang, H. Yang, Z. Wang, H. Jin, Z. Liu, M. M. Olmstead and A. L. Balch, *Angew. Chem., Int. Ed.*, 2009, **48**, 9114–9116.
28 H. Murakami, T. Nomura and N. Nakashima, *Chem. Phys. Lett.*, 2003, **378**, 481–485.
29 A. Satake, Y. Miyajima and Y. Kobuke, *Chem. Mater.*, 2005, **17**, 716–724.
30 A. I. A. Abd El-Mageed and T. Ogawa, *Appl. Surf. Sci.*, 2018, **462**, 904–912.
31 K. B. Ghiassi, M. M. Olmstead and A. L. Balch, *Chem. Commun.*, 2013, **49**, 10721–10723.
32 J. A. Shelnutt, X.-Z. Song, J.-G. Ma, S.-G. Jia, W. Jentzen and C. J. Medforth, *Chem. Soc. Rev.*, 1998, **27**, 31–41.

33 K. M. Steed and J. W. Steed, *Chem. Rev.*, 2015, **115**, 2895–2933.
34 C. P. Brock and R. Taylor, *Acta Crystallogr., Sect. B: Struct. Sci., Cryst. Eng. Mater.*, 2020, **76**, 630–642.
35 E. F. Meyer Jr., *Acta Crystallogr., Sect. B: Struct. Crystallogr. Cryst. Chem.*, 1972, **28**, 2162–2167.
36 D. L. Cullen and E. F. Meyer Jr., *J. Am. Chem. Soc.*, 1974, **96**, 2095–2102.
37 T. D. Brennan, W. R. Scheidt and J. A. Shelnutt, *J. Am. Chem. Soc.*, 1988, **110**, 3919–3924.
38 I. Bernal, CSD communication, CAMJIM, CCDC 644767.†
39 H. M. Lee, M. M. Olmstead, T. Suetsuna, H. Shimotani, N. Dragoe, R. J. Cross, K. Kitazawa and A. L. Balch, *Chem. Commun.*, 2002, 1352–1353.
40 B. Q. Mercado, N. Chen, A. Rodriguez-Fortea, M. A. Mackey, S. Stevenson, L. Echegoyen, J. M. Poblet, M. M. Olmstead and A. L. Balch, *J. Am. Chem. Soc.*, 2011, **133**, 6752–6760.
41 M. Asano, Y. Kaizu and H. Kobayashi, *J. Chem. Phys.*, 1988, **89**, 6567–6576.
42 R. N. S. van der Haas, R. L. P. de Jong, M. Noushazar, K. Erkelens, T. G. M. Smijs, Y. Liu, P. Gast, H. J. Schuitmaker and J. Lugtenburg, *Eur. J. Org. Chem.*, 2004, 4024.
43 G. D. Dorough, J. R. Miller and F. M. Huennekens, *J. Am. Chem. Soc.*, 1951, **73**, 4315.
44 *SAINT and SADABS*, Bruker AXS Inc., Madison, WI, 2018.
45 G. M. Sheldrick, *Acta Crystallogr., Sect. A: Found. Adv.*, 2015, **71**, 3–8.
46 G. M. Sheldrick, *Acta Crystallogr., Sect. C: Struct. Chem.*, 2015, **71**, 3–8.